

Nonlinearity-assisted quantum tunneling in a matter-wave interferometer

Chaohong Lee, Elena A. Ostrovskaya and Yuri S. Kivshar

Nonlinear Physics Centre and ARC Centre of Excellence for Quantum-Atom Optics,
Research School of Physical Sciences and Engineering, Australian National
University, Canberra ACT 0200, Australia

Abstract. We investigate the *nonlinearity-assisted quantum tunneling* in a matter-wave interferometer, which is realised by the adiabatic transformation of a double-well potential into a single-well one. In contrast to the linear quantum tunneling induced by the crossing (or avoided crossing) of neighbouring energy levels, the quantum tunneling between different nonlinear eigenstates is assisted by the nonlinear mean-field interaction. When the barrier between the wells decreases, the mean-field interaction aids quantum tunneling between the ground and excited nonlinear eigenstates. The resulting *non-adiabatic evolution* depends on the input states. The tunneling process leads to the generation of dark solitons, and the number of the generated dark solitons is highly sensitive to the matter-wave nonlinearity. The results of the numerical simulations of the matter-wave dynamics are successfully interpreted with a coupled-mode theory for multiple nonlinear eigenstates.

PACS numbers: 03.75.Lm, 39.20.+q, 03.75.Kk

Submitted to: *J. Phys. B: At. Mol. Opt. Phys.*

1. Introduction

Matter-wave interferometry involves the coherent manipulation of the external or internal degrees of freedom of massive particles [1, 2]. Utilizing the well-developed techniques of trapping and cooling, the matter-wave interferometers have been realised with atomic Bose-Einstein condensates (BECs) [3, 4, 5, 6]. Almost all BEC interferometers based upon spatial interference measure the phase coherence by merging two initially separated condensates [3, 4, 5, 6]. To recombine two condensates confined in a double-well potential, one has to transform the double-well potential into a single-well potential by decreasing the barrier height.

Intrinsic interparticle interactions in atomic condensates have stimulated various studies of the nonlinear behaviour of condensed atoms [7]. A balance between matter-wave dispersion and nonlinear interaction supports a number of nontrivial collective excitations, including bright solitons in condensates with attractive interactions [8, 9] and dark solitons in condensates with repulsive interactions [10, 11]. It was demonstrated that the nonlinearity has important effects on BEC interferometers [12]. The nonlinear excitations in BEC interferometers with repulsive interparticle interaction lead to the generation of dark solitons [13, 14], and it can be utilised to enhance the phase sensitivity of the devices [14, 15].

In a harmonically trapped condensate with repulsive interparticle interactions, the nodes of excited nonlinear eigenstates correspond to dark solitons [16], so that the formation of dark solitons can be associated with populating excited states [16, 17]. Several methods of condensate excitation have been suggested, the most experimentally appealing ones involving time-dependent modifications of trapping potentials [18]. The operation of BEC interferometers and splitters based on spatiotemporal Y- and X-junctions [12, 14] is greatly affected by the possibility of nonlinear excitations. The mechanisms for population transfer between different eigenstates of a trapped BEC explored extensively include non-adiabatic processes [12], Josephson tunneling [19, 20] and Landau-Zener tunneling [21, 22, 23], which are also responsible for population transfer in linear systems. However, in a sharp contrast to linear systems, the quantum tunneling between different nonlinear eigenstates can be assisted by the nonlinear mean-field interaction even in the absence of crossing (and avoided crossing) of the energy levels. Up to now, this peculiar type of quantum tunneling remains poorly explored.

In this paper, we explore the intrinsic mechanism for the quantum tunneling assisted by repulsive nonlinear mean-field interactions in a matter-wave interferometer. We consider the dynamical recombination process of a BEC interferometer, in which an initially deep one-dimensional (1D) double-well potential is slowly transformed into a single-well harmonic trap. Our numerical simulations, employing a time-dependent 1D mean-field Gross-Pitaevskii (GP) equation, show that multiple moving dark solitons are generated as a result of the nonlinearity-assisted quantum tunneling between the ground and excited nonlinear eigenstates of the system, and the qualitative mechanism is independent on the particular shape of the double-well potential. Furthermore, the

number of the generated dark solitons is found to be highly sensitive to the strength of the effective nonlinearity that in turn depends on the total number of condensed atoms and the atom-atom s-wave scattering length. The population transfer between different nonlinear eigenstates caused by the nonlinearity-assisted quantum tunneling can be quantified by a coupled-mode theory for multiple nonlinear eigenstates of the system.

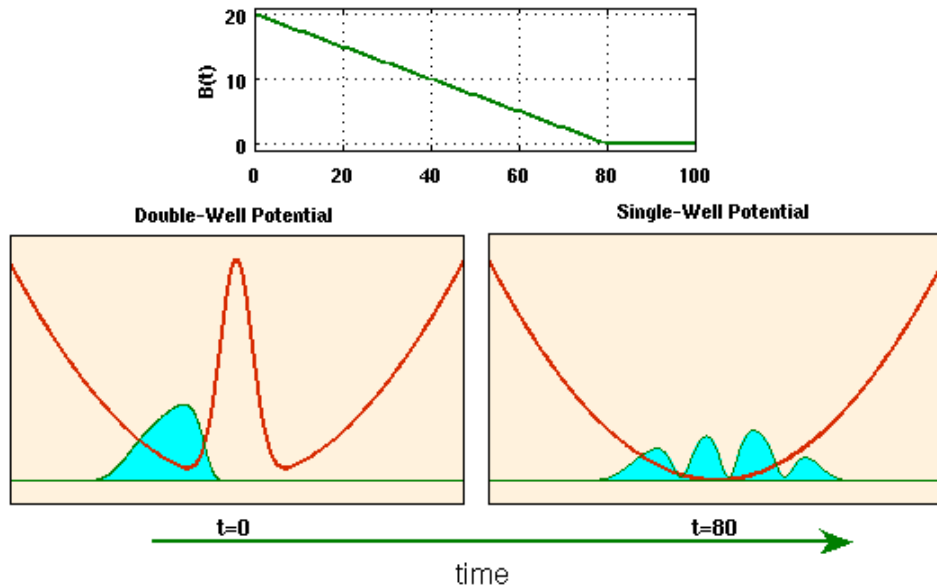


Figure 1. Schematic diagram. Top: time-dependence of the barrier height $B(t)$. Bottom left: initial BEC density distribution (shaded) at $t = 0$ in the double-well potential (solid line). Bottom right: density distribution (shaded) at $t = 80$ in the single-well potential (solid line).

2. Model and numerical results

We consider a condensate under strong transverse confinement, $m\omega_\rho^2(y^2 + z^2)/2$, so that the 3D mean-field model can be reduced to the following 1D model [24]:

$$i\hbar \frac{\partial}{\partial t} \Psi(x, t) = H_0 \Psi(x, t) + \lambda |\Psi(x, t)|^2 \Psi(x, t), \quad (1)$$

where $H_0 = -(\hbar^2/2m)(\partial^2/\partial x^2) + V(x, t)$, m is the atomic mass, $\lambda > 0$ characterizes the effective nonlinearity which we assume to be *repulsive*, and $V(x, t)$ is an external potential. If the condensate order parameter $\Psi(x, t)$ is normalised to one, the effective nonlinearity $\lambda = 2Na_s\omega_\rho\hbar$ is determined by the total number of atoms N , the s-wave scattering length a_s and the transverse trapping frequency ω_ρ [25]. In what follows we use the dimensionless version of the model equation obtained by choosing the natural units of $m = \hbar = 1$.

We assume the time-dependent potential $V(x, t)$ as a spatiotemporal Y-shape potential generated by the superposition of a 1D time-independent harmonic potential

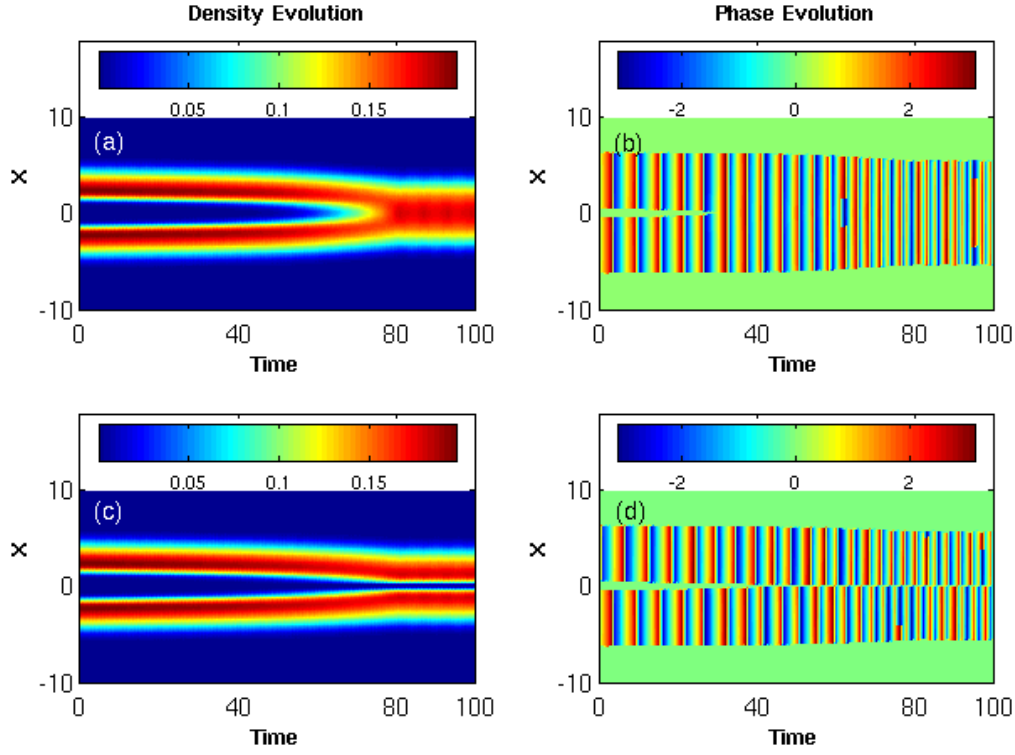


Figure 2. Evolution of the condensate density (left) and phase (right) of the ground and first-excited states for the system of the effective nonlinearity $\lambda = 20$. The first and second rows correspond to the evolution of the ground and first-excited states, respectively.

and a time-dependent Gaussian barrier (see Fig. 1):

$$V(x, t) = \frac{1}{2}\omega^2 x^2 + B(t) \cdot \exp\left(-\frac{x^2}{2d^2}\right), \quad (2)$$

where ω is the trapping frequency, d is the barrier width, and the barrier height depends on time as follows:

$$B(t) = \begin{cases} B_0 - \alpha t, & \text{for } t < B_0/\alpha, \\ 0, & \text{for } t \geq B_0/\alpha, \end{cases} \quad (3)$$

where α is the ramping rate. When the barrier height $B(t) > \omega^2 d^2$, the time-dependent potential is a double-well potential with two minima at $x = \pm d\sqrt{2 \ln[B_0/(d^2\omega^2)]}$. Thus, the 1D description is valid for weak longitudinal confinements satisfying $\omega^{\text{db}} = \omega\sqrt{2 \ln[B_0/(d^2\omega^2)]} \ll \omega_\rho$ and $\omega \ll \omega_\rho$. To ensure the adiabatic evolutions of the symmetric and antisymmetric initial eigenstates, the sweeping rate α must be sufficiently small. In Fig. 2, we show the evolutions of the ground and first-excited eigenstates of the system of effective nonlinearity $\lambda = 20$ and ramping rate $\alpha = 1/4$. For such a small sweeping rate, the ground and first-excited eigenstates for the initial double-well potential both adiabatically evolve to the corresponding ground and first-excited eigenstates for the final single-well potential. This means that the *non-adiabatic effects are negligible* for such a slowly varying process.

The usual double-well BEC interferometers involve condensates trapped in a double-well potential before recombination. Below, we consider the case of the initial state of the BEC being fully localised in a single well of a symmetric double-well potential with a sufficiently high barrier, so that there is *no significant overlap* between the Wannier states of the two wells. The fully localised initial state can be viewed as the equal-probability superposition of the ground and first-excited eigenstates, so that it can be used to observe the interference of these two eigenstates [26]. For BECs trapped in such a deep potential, the mean-field ground and first excited states are degenerate or quasi-degenerate. Even for low barriers, if the tight-binding condition is still satisfied, the two-mode approximation will give the picture of a classical Bose-Josephson junction. In the framework of second quantisation, the system obeys a two-site Bose-Hubbard Hamiltonian. In this fully quantum picture, a completely localised initial state corresponds to the highest excited state for repulsive interactions. This state shows degeneracy with the sub-highest excited state [27], which corresponds to the bistability in a classical Bose-Josephson junction [28].

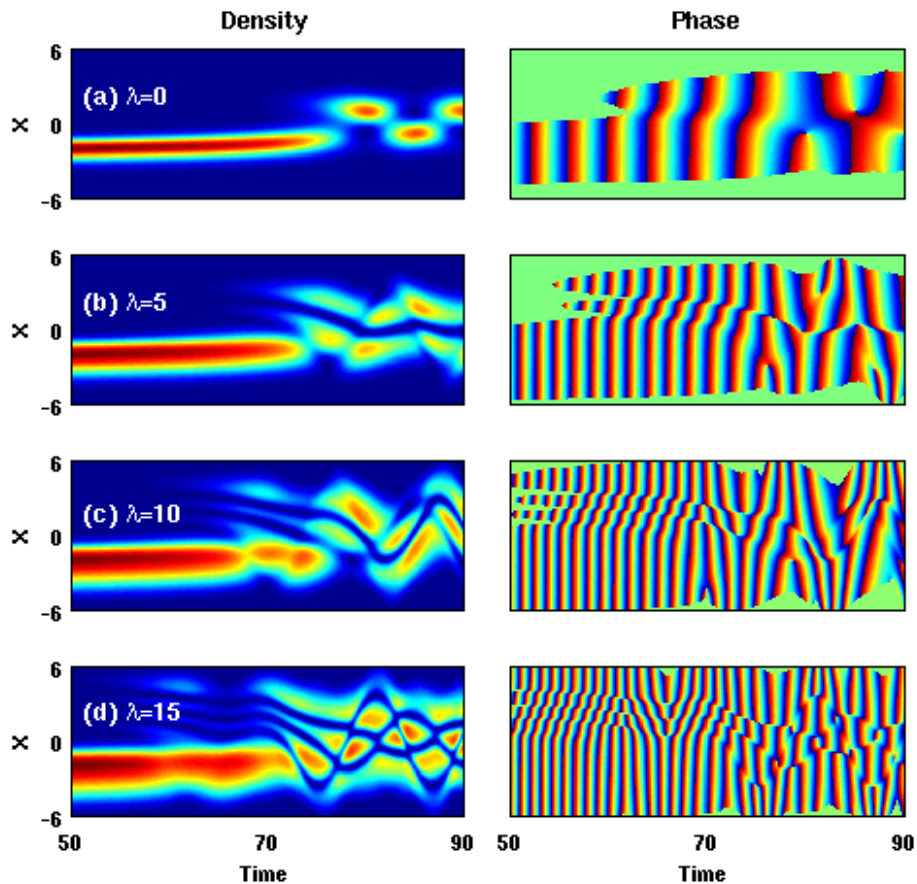


Figure 3. Evolution of the condensate density (left) and phase (right) for different values of the effective nonlinearity λ . Cases (a-d) correspond to $\lambda = 0, 5, 10$ and 15 , respectively.

Since initially there is no overlap between the two Wannier states, the quantum tunneling between those states is negligible. As the barrier height gradually decreases, the overlap between two Wannier states becomes more significant. Then both the quasi-degeneracy between the ground and first excited states in the mean-field picture and the quasi-degeneracy between the highest excited and sub-highest excited states in the quantum picture break down. The quantum tunneling of the fully localised state becomes more pronounced as the barrier height is decreasing.

In Fig. 3, we show the time evolution of the condensate density and phase for the trapping frequency $\omega = 0.2\pi$, the initial barrier height $B_0 = 20.0$, the barrier width $d = \sqrt{2}/2$, the ramping rate $\alpha = 1/4$, and different values of the effective nonlinearity λ . To explore the dynamic evolution, we numerically integrate the GP equation with the well-developed operator-splitting procedure and the absorbing boundary conditions. For the settled small sweeping rate, all symmetric (antisymmetric) states for the deep double-well potential will adiabatically evolve to the corresponding ground (or excited) states for the single-well potential.

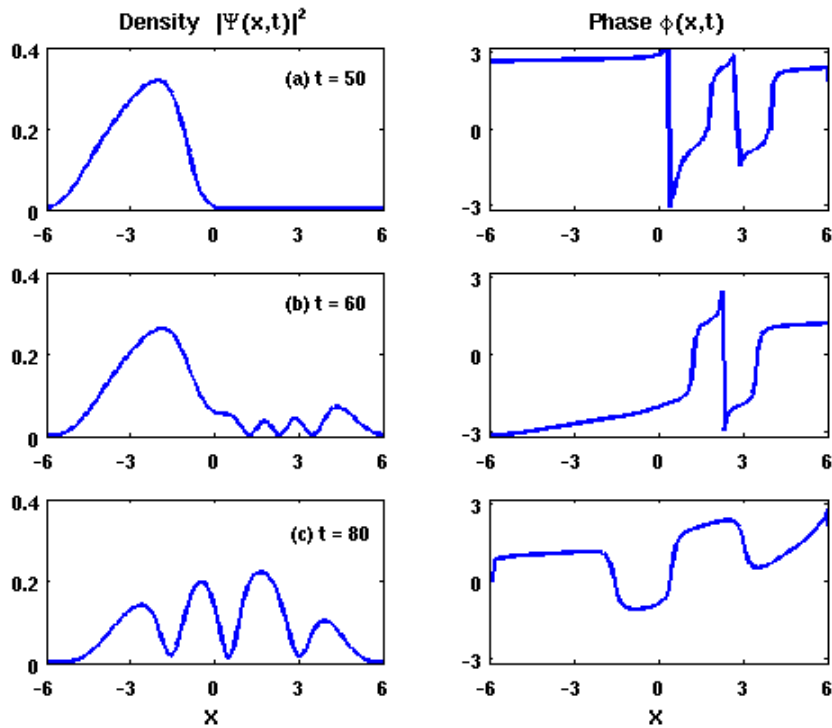


Figure 4. Formation of dark solitons in the system with the effective nonlinearity $\lambda = 15$. Left: density distributions $|\Psi(x,t)|^2$ for different times. Right: phase distributions $\phi(x,t)$ for the corresponding density distributions.

Evolution of the fully localised initial state strongly depends on the values of the effective nonlinearity λ . For the linear case ($\lambda = 0$), the fully localised initial state can be viewed as the equal-probability superposition of the symmetric and antisymmetric states, so that the evolving state is always the equal-probability superposition of the

ground and the first excited states of the system, according to the adiabatic theorem. Due to the nonlinear interactions, the superposition principle becomes invalid, and the resulting behavior can be interpreted as the coupled dynamics of the ground and multiple excited states of the nonlinear system. Akin to the linear systems, the quantum tunneling appears once the quasi-degeneracy between the ground and the first excited state is broken, and gradually becomes significant with decreasing barrier height. The time scale on which the quantum tunneling appears in the nonlinear system decreases with the nonlinear interaction strength λ . The excited nonlinear states of the BEC in a single-well potential can be thought as stationary configurations of single or multiple dark solitons [16]. As a result of the population transfer to such excited modes, the condensate develops multi-peak distribution with significant phase steps across density notches between neighboring peaks. These notches are dark or gray solitons with well-defined phase steps close to π (see Fig. 4).

The number of dark solitons formed in this process shows strong dependence on the effective nonlinearity λ , see Fig. 5. This dependence exhibits multiple plateaus as one changes the effective nonlinearity λ , as shown in Fig. 5. Given the dependence of the nonlinear interaction strength on the key parameters of the system, $\lambda = 2Na_s\omega\rho\hbar$, one can control the number of generated solitons by adjusting the s-wave scattering length with the Feshbach resonance, the total number of atoms in the condensate with initial preparation, and/or the transverse trapping frequency with tuning the transverse trapping field strength.

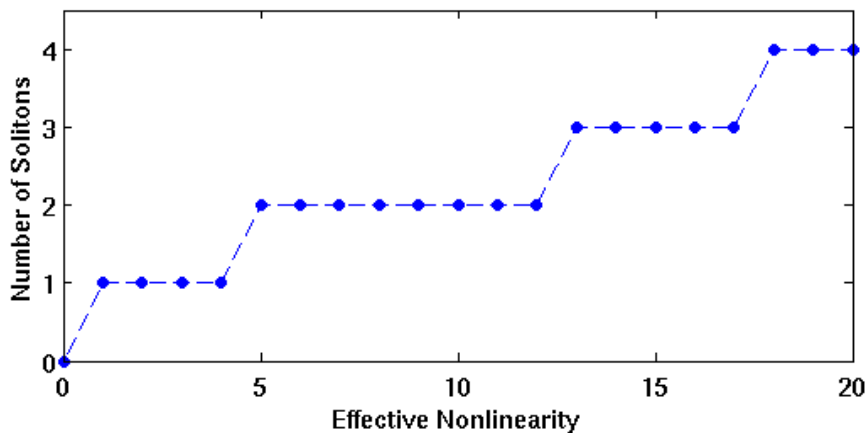


Figure 5. Number of dark solitons generated in the condensate at $t = 80$ versus the effective nonlinearity parameter λ .

3. Modal decomposition

To obtain the quantitative picture of the population transfer, we decompose an arbitrary state of our time-dependent system as [15, 29],

$$\Psi(x, t) = \sum_j^N C_j(t) \phi_j(x, t), \quad (4)$$

where $\phi_j(x, t)$ is the j -th stationary state for the nonlinear system with the potential $V(x, t)$, which obeys the (dimensionless) equation:

$$\mu_j(t) \phi_j(x, t) = \left[-\frac{1}{2} \frac{d^2}{dx^2} + V(x, t) \right] \phi_j(x, t) + \lambda \phi_j^3(x, t). \quad (5)$$

Here, $\mu_j(t)$ is the chemical potential for the j -th stationary state. The stationary states $\phi_j(x, t)$ generalise the eigenstates of the linear system to the case of the nonlinear interactions, and they can be termed ‘nonlinear eigenstates’.

The population dynamics of different nonlinear eigenstates can be described by the evolution of the complex coefficients $C_j(t)$, which obey a series of coupled first-order differential equations,

$$i \frac{dC_l(t)}{dt} = \sum_j^N \left[E_0^{l,j} + \sum_{k,k'} Q_{k,k'}^{l,j} C_k^*(t) C_{k'}(t) \right] C_j(t). \quad (6)$$

Due to the conservation of the total number of particles, $C_j(t)$ satisfy the normalisation condition $\sum_j |C_j(t)|^2 = 1$. Here the linear coupling parameters are

$$E_0^{l,j}(t) = \int \phi_l^*(x, t) H_0 \phi_j(x, t) dx, \quad (7)$$

and the nonlinear coupling parameters are

$$Q_{k,k'}^{l,j}(t) = \lambda \int \phi_l^*(x, t) \phi_k^*(x, t) \phi_{k'}(x, t) \phi_j(x, t) dx. \quad (8)$$

For a spatially symmetric potential $V(x, t) = V(-x, t)$, we have $Q_{k,k'}^{l,j}(t) = 0$, and then $(k + k' + l + j)$ are odd integer numbers.

In our numerical simulations, we generalise the direct relaxation method for linear quantum systems [30] to calculate the eigenstates and their eigenvalues (chemical potentials) for our nonlinear system with different effective nonlinearities at any moment of time. Projecting the condensate wavefunction $\Psi(x, t)$ onto the nonlinear eigenstates $\phi_j(x, t)$, we find the population probabilities $P_j(t) = |C_j(t)|^2 = \left| \int \phi_j^*(x, t) \Psi(x, t) dx \right|^2$ which depend on the time and the effective nonlinearity λ .

In Fig. 6(a), we show the time evolution of the population probabilities $P_j(t)$ for the effective nonlinearity $\lambda = 2.0$. Here we only consider four lowest eigenstates (i.e., $N = 4$), so that P_0 is the ground state population probability, P_j ($j = 1, 2, 3$) are the population probabilities of the j -th excited state, and $P_{\text{tot}} = P_0 + P_1 + P_2 + P_3$ is the total probability of the first four eigenstates. For $t < 50$, the population probabilities keep almost unchanged. In the region of $50 < t < 80$, we observe a fast population transfer from the ground state to the first excited state. After the recombination of

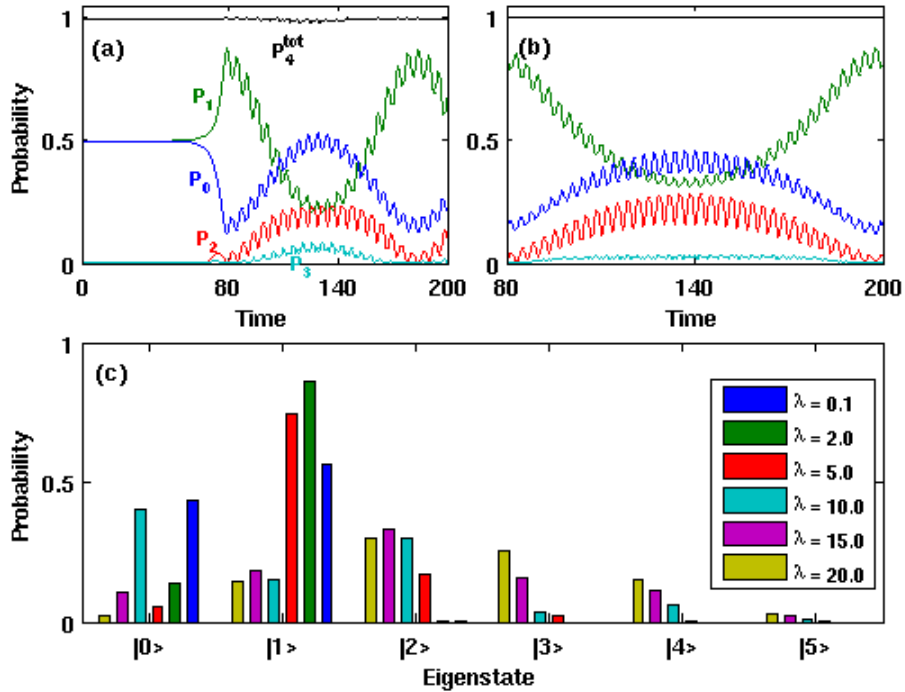


Figure 6. (a) Time evolution of population probabilities in different eigenstates for $\lambda = 2$, where P_0 and P_j ($j = 1, 2, 3$) are the population probabilities of the ground state and the j -th excited state, respectively. The total probability of the first four eigenstates is denoted as $P_{tot} = P_0 + P_1 + P_2 + P_3$. (b) The corresponding population evolution for $t > 80$ obtained from the coupled-mode equation (6) with first four lowest eigenstates. (c) Population probabilities for the first six lowest nonlinear eigenstates at $t = 80$.

the two wells, i.e. for $t > 80$, the populations in different eigenstates oscillate with time although the system has a time-independent potential and no degeneracy between neighbouring energy levels. This differs drastically from the linear dynamics where the populations in different eigenstates always stay unchanged. We find that at this value of the effective nonlinearity the total population probability $P_{tot}(t)$ in the first four eigenstates is always close to one. The low-frequency population oscillations are dominated by the linear coupling between different modes and the high-frequency ones are due to the nonlinear cross-coupling of the nonlinear modes.

For small λ , the dynamics of P_j after the merging of the two wells can be approximately captured by the projection of the BEC state at the moment of the merging (here $t = 80$) onto the set of N stationary nonlinear states $\phi_j(x)$ of the single-well potential $V_0(x)$ of $B(t) = 0$. This is confirmed in Fig. 6(b), where we employ the coupled-mode theory (6) with $N = 4$ eigenstates of $V_0(x)$ [cf. Fig. 6(a)]. The number of eigenstates, N , that must be considered in the coupled-mode theory, increases with the effective nonlinearity. The highest-order mode ($j = N$) of the harmonic potential $V_0(x)$ with significant (non-zero) excitation probability P_N at the merging time will therefore

determine the number N of dark solitons that are likely to be formed. Figure 6(c) shows the excitation probabilities at $t = 80$ for the first six lowest eigenstates of $V_0(x)$ and different λ . By comparing the number of significantly excited states for different values of λ , one can see that the number of dark solitons formed is indeed approximately determined by the highest-excited nonlinear mode of the harmonic trap that is still sufficiently populated. For instance, $N = 1$ solitons are expected to form for $\lambda = 2$, and $N = 2$ for $\lambda = 10$ (cf. Fig. 5).

4. Conclusions

We have explored the nonlinearity-assisted quantum tunneling in the dynamical recombination process of a BEC interferometer. In contrast to the Josephson tunneling and Landau-Zener tunneling, the nonlinearity-assisted quantum tunneling is brought about by the nonlinear inter-mode population exchange scattering. The excitations caused by this type of tunneling lead to the dark soliton generation in the process that differs dramatically from the phase imprinting [10, 11] or condensates collisions [13]. The number of generated solitons can serve as a sensitive measure of the degree of the nonlinearity in the system. With the well-developed techniques for preparing and manipulating condensed atoms in double-well potentials [3, 4, 5, 6], loading the condensed atoms in one well of a deep double-well potential and adjusting the barrier height, the experimental realisation of this scheme seems feasible.

Note added: After this manuscript was prepared for submission, the group of Peter Engels from the Washington State University reported the experimental observation of matter-wave dark solitons due to quantum tunneling [31], in the process of sweeping a high potential barrier from one edge of the trap to the other.

The authors thank R. Gati and M. Oberthaler for stimulating discussions. This work was supported by the Australian Research Council (ARC).

References

- [1] Berman P 1997 *Atom Interferometry* (Academic Press, San Diego)
- [2] Chu S 2002 *Nature* **416** 206
- [3] Shin Y, Saba M, Pasquini TA, Ketterle W, Pritchard DE, and Leanhardt AE 2004 *Phys. Rev. Lett.* **92** 050405
- [4] Albiez M, Gati R, Fölling J, Hunsmann S, Cristiani M, and Oberthaler MK 2005 *Phys. Rev. Lett.* **95** 010402
- [5] Schumm T, Hofferberth S, Andersson LM, Wildermuth S, Groth S, Bar-Joseph I, Schmiedmayer J, and Krüger P 2005 *Nature Phys.* **1** 57
- [6] Hall BV, Whitlock S, Anderson R, Hannaford P, and Sidorov AI 2007 *Phys. Rev. Lett.* **98** 030402
- [7] Rolston SL and Phillips WD 2002 *Nature* **416** 219
- [8] Khaykovich L, Schreck F, Ferrari G, Bourdel T, Cubizolles J, Carr LD, Castin Y, and Salomon C 2002 *Science* **296** 1290
- [9] Strecker KE, Partridge GB, Truscott AG, and Hulet RG 2002 *Nature* **417** 150
- [10] Burger S, Bongs K, Dettmer S, Ertmer W, Sengstock K, Sanpera A, Shlyapnikov GV, and Lewenstein M 1999 *Phys. Rev. Lett.* **83** 5198

- [11] Denschlag J, Simsarian JE, Feder DL, Clark CW, Collins LA, Cubizolles J, Deng L, Hagley EW, Helmerson K, Reinhardt WP, Rolston SL, Schneider BI, and Phillips WD 2000 *Science* **287** 97
- [12] Stickney JA and Zozulya AA 2003 *Phys. Rev. A* **68** 013611
- [13] Reinhardt WR and Clark CW 1997 *J. Phys. B: At. Mol. Opt. Phys.* **30** L785
- [14] Jo GB, Choi JH, Christensen CA, Pasquini TA, Lee YR, Ketterle W, and Pritchard DE 2007 *Phys. Rev. Lett.* **98** 180401
- [15] Negretti A and Henkel C 2004 *J. Phys. B: At. Mol. Opt. Phys.* **37** L385
- [16] Kivshar YS, Alexander TJ, and Turitsyn SK 2001 *Phys. Lett. A* **278** 225
- [17] Yukalov VI, Yukalova EP, and Bagnato VS 1997 *Phys. Rev. A* **56** 4845
- [18] Damski B, Karkuszewski ZP, Sacha K, and Zakrzewski J 2001 *Phys. Rev. A* **65** 013604
- [19] Smerzi A, Fantoni S, Giovanazzi S, and Shenoy SR 1997 *Phys. Rev. Lett.* **79** 4950
- [20] Lee C, Hai W, Shi L, Zhu X, and Gao K 2001 *Phys. Rev. A* **64** 053604
- [21] Liu J, Fu LB, Ou BY, Chen SG, Choi DI, Wu B, and Niu Q 2002 *Phys. Rev. A* **66** 023404
- [22] Liu J, Wu B, and Niu Q 2003 *Phys. Rev. Lett.* **90** 170404
- [23] Witthaut D, Graefe EM, and Korsch HJ 2006 *Phys. Rev. A* **73** 063609
- [24] Perez-Garcia VM, Michinel H, and Herrero H 1998 *Phys. Rev. A* **57** 3837
- [25] Carr LD and Brand J 2004 *Phys. Rev. Lett.* **92** 040401
- [26] Praviate communications with Li-Bin Fu, the details will be published elsewhere.
- [27] Lee C 2006 *Phys. Rev. Lett.* **97** 150402
- [28] Lee C, Hai W, Shi L, and Gao K 2004 *Phys. Rev. A* **69** 033611
- [29] Ostrovskaya EA, Kivshar YS, Lisak M, Hall B, Cattani F, and Anderson D 2000 *Phys. Rev. A* **61** 031601(R)
- [30] Kosloff R and Tal-Ezer H 1986 *Chem. Phys. Lett.* **127** 223
- [31] Engels P and Atherton C 2007 Preprint arXiv:0704.2427v1 [cond-mat.other]